**Figure 2** Electrophysiological findings for motor symptoms of the monkeys. (**A**) Compound muscle action potentials (CMAPs) in the thenar muscle after stimulation of the median nerve at the wrist. They gradually decreased in size, and became inexcitable in the late stage. There was no change of compound muscle action potential size in the control monkey. (**B**) Ratio of the compound muscle action potential size 3–5 days after the onset (early stage) or 2–5 weeks after the onset (late stage) to the size before injection. In the early stage, there was no reduction in compound muscle action potential size on the contralateral side, but moderately attenuated in the late stage. (**C**) Needle EMG findings of the forearm muscle. Circles indicate fasciculation potentials; open triangles, positive sharp waves; filled triangles, fibrillation potentials.

most motoneurons in the lateral nuclear group of the anterior horn. In contrast, almost all neurons in other areas of the spinal cord including the posterior horn showed flag signal of exogenously expressed TDP-43 only in the nucleus (Fig. 4A and D). Importantly, the contralateral lateral nuclear group also exhibited TDP-43 mislocalization on the side of forelimb that did not yet show obvious motor symptoms (Supplementary Fig. 6). Signals of exogenous Flag-TDP-43 were detected by real-time polymerase chain reaction on the contralateral half of the spinal cord (Supplementary Fig. 7). However, this distribution indicates that this regional selectivity is not due to differences in the concentration of the injected AAV, but rather is due to properties of the affected neurons. In the late stage, 2–5 weeks after onset, the percentage of motoneurons with TDP-43 mislocalization decreased ~47% in the lateral nuclear group, and was <2% in the ventromedial nuclear group (Figs 3B and 4D). The number of large motoneurons ($\geqslant 20\,\mu m$) in the early stage in this lateral nuclear group did not change, but in the late stage, was reduced by ~42% (Fig. 4B, C and E). In contrast,

the reduction in the number of large neurons in the ventromedial nuclear group was not significant (control, 1.78 ± 0.20 versus TDP-43, 1.68 ± 0.18/section, $P = 0.80$). Astrogliosis was also more prominent in the lateral area than in the ventromedial area of the anterior horn (data not shown). Motoneuronal degeneration of the lateral nuclear group was also confirmed by studying the anterior roots of the eighth cervical segment, which showed frequent myelin ovoids and loss of large myelinated axons ($\geqslant 8\,\mu m$) in the late stage, although they were almost normal in the early stage (Fig. 5A–C). This axonal loss in the anterior roots is consistent with pathological change of the thenar muscle, showing numerous small angulated atrophic fibres (Fig. 5D).

We furthermore examined whether such a regional change of TDP-43 mislocalization occurs in spinal cord of nine patients with ALS with upper limb weakness and hand muscle atrophy. TDP-43 mislocalization was observed much more in the lateral nuclear group than in the ventromedial nuclear group of the cord at the eighth cervical segment (Fig. 6A–C).
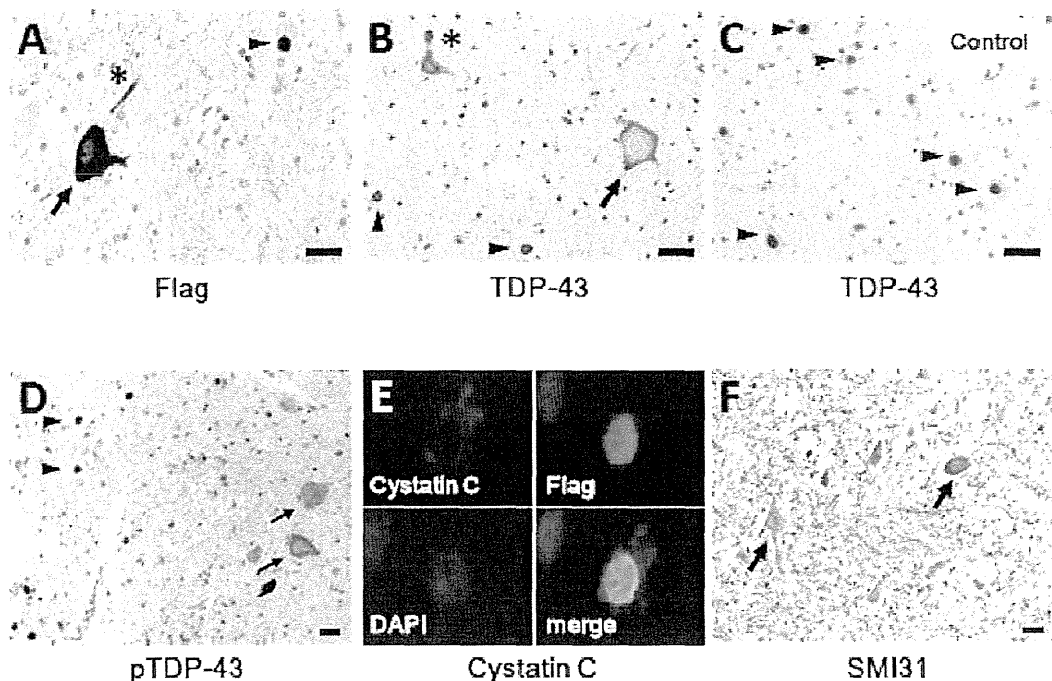
Figure 3 Neuropathological findings of monkey spinal cords of TDP-43–overexpressed monkeys at the late stage (**A, D–F**), and control with mock AAV (**C**). (**A–D**) TDP-43-overexpressed spinal cord immunostaining using antibodies to Flag (**A**), pan-TDP-43 (**B**) and pS409/410 TDP-43 (**D**) demonstrated mislocalization in cytoplasm (arrows), and dystrophic neurites (asterisks) as well as normal localization in nuclei (arrowheads), whereas normal spinal cord showed only nuclear localization of TDP-43. (**E**) Co-labelling of a motoneuron expressing TDP-43 in the nucleus with antibodies to cystatin C (red) and Flag (green). The nucleus is labelled with DAPI. (**F**) Immunostaining using SMI31 revealed the aberrant presence of phosphorylated neurofilament in the neuronal cytoplasm (arrows). Scale bars: 20 μm. Immunostainings of spinal cord with control mock AAV using the antibodies to Flag, pS409/410 TDP-43, cystatin C and SMI31 are shown in Supplementary Fig. 7.

Interspecies differences in TDP-43 pathology in rodents and primates

To investigate interspecies differences in TDP-43 pathology, we injected the identical TDP-43-expressing AAV at the same concentration into rat cervical cords. Expression level of Flag-TDP-43 messenger RNA around the injection site in rat spinal cord was >20-fold higher than that of endogenous TDP-43 level, and this fold change was similar to that in monkey spinal cord (Fig. 7A). Rats injected with TDP-43 AAV showed progressive motor weakness (Fig. 7B), measured by grip strength. Importantly, exogenous TDP-43 was observed only in the nuclei of motoneurons in both early (14 days after injection of AAV) and late (4 weeks after injection of AAV) stages (Fig. 7C). Since mislocalization of TDP-43 in the monkey spinal cords was more prominent in the early stage (14 days), we also examined the pathology of rat spinal cords at a very early stage (7 days); however, the weak Flag immunoreactivity was still limited to the nucleus of motoneurons (data not shown). Furthermore, this rat model failed to exhibit cystatin C-positive aggregates, dystrophic neurites, or aberrant accumulation of phosphorylated neurofilaments in the cytoplasm of spinal motoneurons (Fig. 7D). These neuropathological findings indicate that this rat model was less similar to human ALS

than our monkey model in TDP-43 localization and other characteristic features of ALS.

Detection of the 25-kDa C-terminal fragment and phosphorylated TDP-43 in the early stage

Biochemically, immunoblot analysis of monkey spinal cord demonstrated that the exogenous Flag-tagged TDP-43 became much more insoluble than endogenous TDP-43 (Fig. 8A). The phosphorylation of TDP-43 was unclear in the early stage (Fig. 8B) but clearly detected later (Fig. 8C). Neither a C-terminal nor a phosphospecific TDP-43 antibody detected the 25-kDa C-terminal fragment (Fig. 8A–C). These suggest that neither phosphorylation of TDP-43 or its 25-kDa C-terminal fragment in spinal cord is necessary to initiate motoneuronal dysfunction and degeneration in our monkeys.

Discussion

Frequent mislocalization of TDP-43 in the cytoplasm and loss of its nuclear staining are major pathological hallmarks in the histological
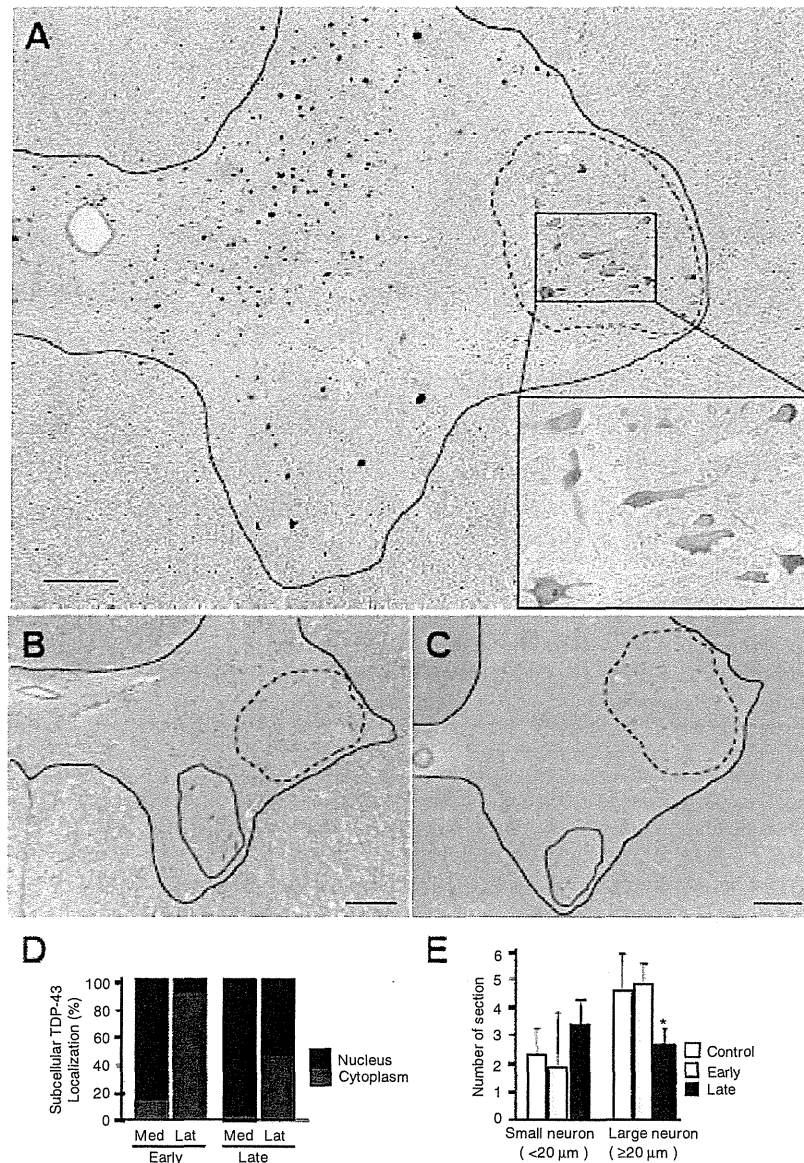
Figure 4 Regional mislocalization of TDP-43 and cell death in monkey spinal cords. (**A**) Sections from the injected side of the eighth cervical segment of the cord taken at the early stage and immunostained with an anti-Flag antibody. Most neurons in the lateral nuclear group (area encircled by broken line) showed cytoplasmic mislocalization of TDP-43 (inset), but almost all neurons in other areas expressed exogenous TDP-43 in the nucleus. Scale bars: 200 μm. (**B** and **C**) The eighth cervical level of cord from monkeys injected with TDP-43–expressing (**B**) and control (**C**) AAV, taken at the late stage and stained with haematoxylin and eosin. The number of large motoneurons decreased in the lateral nuclear group (areas encircled by broken line), but not in ventromedial nuclear group (areas encircled by red solid line). Scale bars: 200 μm. (**D**) Percentage of neurons with nuclear (black) or cytoplasmic (red) localization of exogenous TDP-43 in the lateral nuclear groups on the injected side. Neurodegeneration affects the lateral nuclear group more than the ventromedial nuclear group. (**E**) Cell count of neurons in the lateral nuclear group on haematoxylin and eosin staining. Mean ± SEM. $n = 3$, $*P < 0.05$. Lat = lateral nuclear group; Med = ventromedial nuclear group.

diagnosis of ALS and FTLD (Geser *et al.*, 2010). The classification of TDP-43 proteinopathy is based on a combination of neuronal cytoplasmic inclusions and dystrophic neurites (Mackenzie *et al.*, 2011). The morphological features in our monkeys are close to type B TDP-43 proteinopathy, which is usually observed in the

brains of patients with ALS. The only difference between the pathology of our monkeys and type B TDP-43 proteinopathy is that mislocalized cytoplasmic TDP-43 was usually diffuse and neuronal cytoplasmic inclusions were less frequent in our monkeys. Since this monkey is an acute model for TDP-43 pathology, it possibly
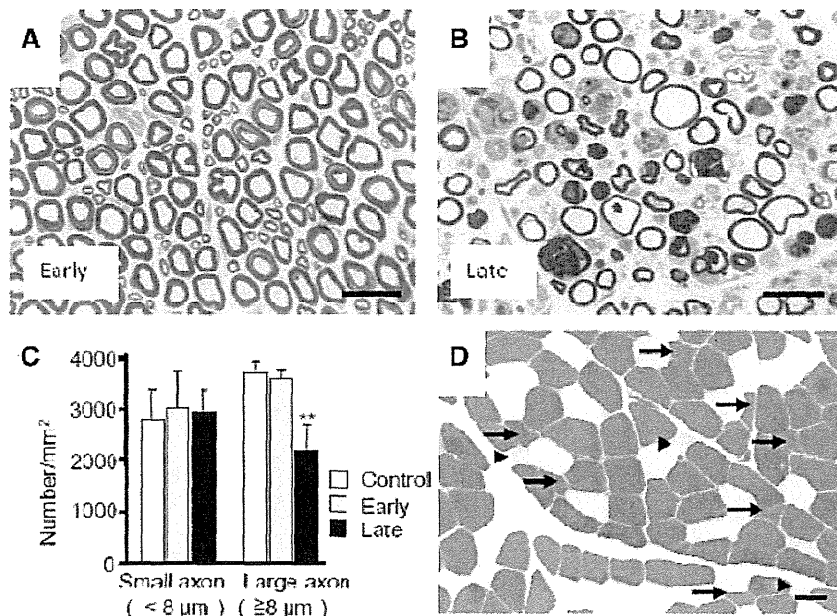
Figure 5 Pathological finding of monkey anterior root and skeletal muscle. Toluidine blue staining of the eighth cervical anterior roots on the injected side in the early (**A**) and late (**B**) stages, and their myelinated axon densities (**C**). Mean ± SEM, $n = 3$, $**P < 0.01$. (**D**) Transverse section of the biceps brachii muscle from a TDP-43–expressing monkey 4 weeks after injection, stained with ATPase (pH 10.6). Small angulated atrophic changes of type I (arrowheads) and type II (arrows) fibres, with predominant involvement of type II fibres, can be seen. Scale bar: 50 μm.

takes more time for diffusely mislocalized TDP-43 to be aggregated. Moreover, in the spinal cords of patients with ALS, diffuse cytoplasmic TDP-43 staining is more common, and neuronal cytoplasmic inclusions are less frequent than in the brain and may even be absent (Giordana *et al.*, 2010). Thus, our monkey model shows the key features of TDP-43 proteinopathy as seen in the ALS spinal cord.

Interestingly, despite the diffuse expression of exogenous TDP-43 in the spinal cord, TDP-43 mislocalization and neuron loss predominantly occurred in the lateral nuclear group in Rexed lamina IX, in which large neurons are mostly α-motoneurons (Carpenter *et al.*, 1983). The sensory neurons and interneurons in laminae III–VIII rarely showed TDP-43 mislocalization, and large motoneurons in the ventromedial nuclear group, most of which are also α-motoneurons, showed much less TDP-43 mislocalization and neuron loss. Within lamina IX, the lateral nuclear group innervates the distal, fast-contracting muscles of the extremities, and the ventromedial nuclear group innervates the posture-related, continuously contracting muscles attached to the axial skeleton (Carpenter *et al.*, 1983). This regional vulnerability among α-motoneurons is consistent with the distal hand or foot muscles being the first involved in 73% of patients with non-bulbar ALS (Harverkamp *et al.*, 1995; Körner *et al.*, 2011) and might be related to axon length, which affects axonal transport (Bilsland *et al.*, 2010), or to the preferential susceptibility of fast-fatigue rather than slow motoneurons (Dengler *et al.*, 1990; Pun *et al.*, 2006). Furthermore, in nine patients with ALS, more

TDP-43 mislocalization was observed in the lateral nuclear group than in the ventromedial nuclear group of the eighth cervical cord segments. Taking these results together, we think that the tropism of TDP-43 mislocalization was similar to that of ALS pathology. However, expression levels of exogenous wild-type TDP-43 in our monkey and rat models were very high ($\sim$20-fold higher than that of endogenous TDP-43), which was partly due to lack of 3'-untranslated region in our TDP-43 expression construct. This is probably because TDP-43 controls its own expression through a negative feedback loop by binding to 3'-untranslated region sequences in its own messenger RNA (Ayala *et al.*, 2010; Polymenidou *et al.*, 2010). The unphysiologically high level of TDP-43 expression in our animal models should be taken into consideration when interpreting our findings.

Since Flag TDP-43 messenger RNA was detected in the spinal cord contralateral to the injected side by real-time polymerase chain reaction analysis, the AAV virus was shown to spread contralaterally through the spinal cord causing motor paresis and reduction of compound muscle action potential size in the opposite forelimb. However, it is still possible that there was concomitant cell-to-cell or trans-synaptic propagation of Flag TDP-43 protein in the spinal cord. Moreover, it is interesting that the Flag-TDP-43 signal was selectively extended into Betz cells in the forelimb area of precentral gyrus contralateral to the injection side, which can be explained by a retrograde progression from α-motoneuron in the cervical cord. More sophisticated experimental paradigms are necessary to distinguish whether it is the AAV vector itself,
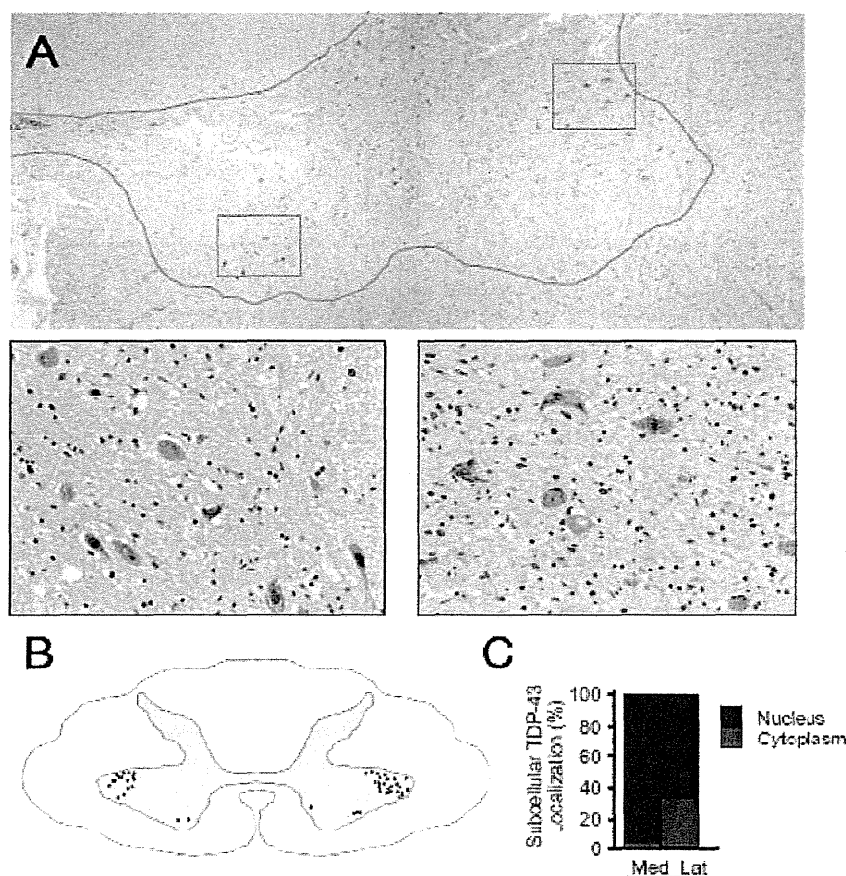
Figure 6 Pan-TDP-43 staining of spinal cords of patients with ALS. (**A**) Autopsied eighth cervical segment of spinal cord immunostained with pan-TDP-43 antibody. Scale bars: 200 μm in **A** and 50 μm in window insets. (**B**) Schematic illustration of the distribution of neurons with TDP-43 mislocalization, made by summing data from five sections (at 20-μm intervals). (**C**) Percentage of neurons with nuclear or cytoplasmic localization of exogenous TDP-43 in the lateral and medial nuclear groups. More frequent TDP-43 mislocalization in the lateral nuclear group in spinal cords of patients with ALS than in the medial nuclear group. Mean ± SEM, $n = 10$, $P < 0.01$. Scale bars: 50 μm. Lat = lateral nuclear group; Med = ventromedial nuclear group.

transcribed messenger RNA or Flag-TDP protein that is the molecule responsible for this progression, which is a prime objective for our future study.

Bunina bodies are small, cystatin C-positive, eosinophilic cytoplasmic inclusions and are generally considered a specific hallmark of sporadic ALS (Okamoto et al., 1993; Mitsumoto et al., 1998). Importantly, Bunina bodies are absent in familial ALS that is due to the SOD1 mutation (Tan et al., 2007) or FUS/TLS mutation (Tateishi et al., 2010), but they have been detected in familial ALS with the TDP-43 mutation (Yokoseki et al., 2008) as well as in sporadic ALS. These imply an association between Bunina bodies and TDP-43 pathology in sporadic ALS. From this point of view, the generation of cystatin C-positive cytoplasmic aggregates in our monkeys might strengthen their pathological value as a model of sporadic ALS.

Biochemically, TDP-43 proteinopathy is characterized by decreased solubility, phosphorylation and the generation of 25-kDa C-terminal fragment (Arai et al., 2006; Neumann et al.,

2006; Hasegawa et al., 2008). In TDP-43-overexpressing monkeys, the exogenous TDP-43 became much more insoluble than endogenous TDP-43 of control monkeys, indicating that expression of large amounts of exogenous wild-type TDP-43 can render it insoluble. Unexpectedly, the solubility of endogenous monkey TDP-43 did not become insoluble in TDP-43-overexpressing monkeys. The expectation would be that exogenous insoluble TDP-43 would recruit endogenous monkey TDP-43 and alter its solubility. In this biochemical aspect of TDP-43 solubility, our monkey model differs from patients with ALS.

The pathological role of phosphorylated TDP-43 is still unclear; TDP-43 phosphorylation in culture cells enhances its oligomerization (Hasegawa et al., 2008), but experiments with a phosphorylation-resistant mutant TDP-43 indicated that phosphorylation is not required for inclusion formation or cellular toxicity (Zhang et al., 2009). In our monkeys, phosphorylation of TDP-43 was a late event but not observed at 4 days after symptom onset. This finding suggests that TDP-43 phosphorylation is not
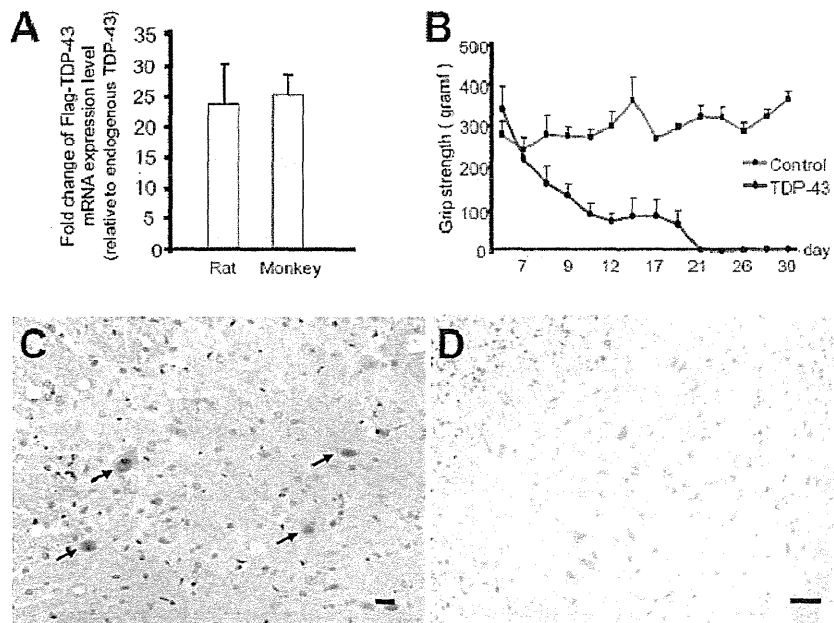
Figure 7 Effect of TDP-43-expressing AAV in rat spinal cords. (**A**) Ratio of exogenously expressed Flag-TDP-43 messenger RNA level to endogenous rat or cynomolgus TDP-43 messenger RNA level evaluated by quantitative real-time polymerase chain reaction.
Mean ± SEM, rat, n = 4; cynomolgus, n = 3, P = 0.74. (**B**) Time course of grip strength. Mean ± SEM. (**C**) Nuclear staining of exogenous TDP-43 in cervical cord sections of AAV-injected rats by immunostaining with an anti-Flag antibody (arrows). (**D**) Immunostaining of cervical cord sections of TDP-43–expressing rat, 4 weeks after injection, with SMI31 did not show aberrant phosphorylated neurofilament in the neuronal cytoplasm. Scale bars: 20 μm.
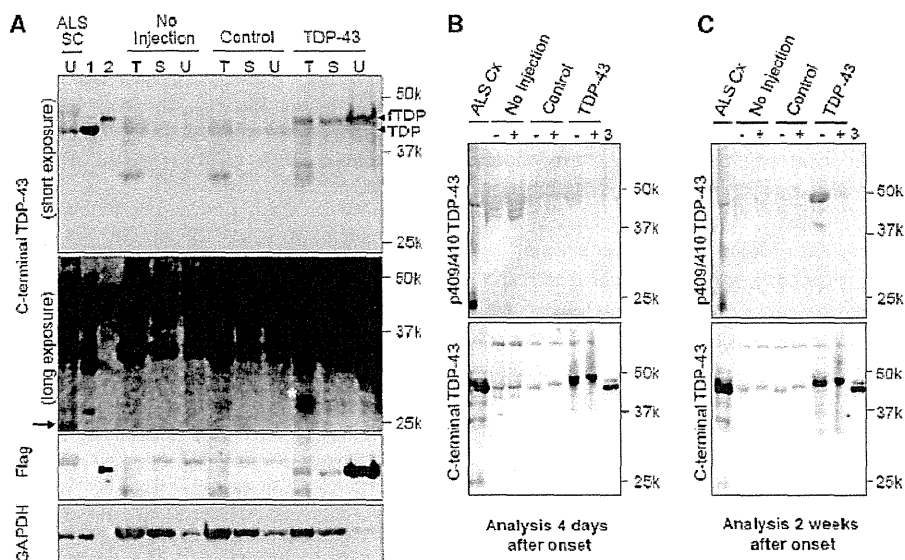
Figure 8 Biochemical analysis of monkey spinal cords. (**A**) Immunoblot of cervical spinal cord lysates from TDP-43–expressing monkeys (4 weeks after injection) and patients with ALS using antibodies recognizing the C-terminus of TDP-43 and Flag. SC = spinal cord of patient with ALS; 1 = TDP-43–expressing HEK 293T cell lysate; 2 = Flag-TDP-43–expressing HEK 293T cell lysate; T = 1% Triton X-100-soluble; S = 1% sarkosyl-soluble; U = 8 mol/l urea-soluble fraction; fTDP = Flag-TDP-43. A longer exposure (second panel from *top*) revealed the 25-kDa C-terminal fragment in the spinal cord of a patient with ALS (arrow). The ~30-kDa band noted in the Triton-soluble fraction from the spinal cord of a TDP-43–expressing monkey (asterisk) was different from the 25-kDa C-terminal fragment (arrow). (**B** and **C**) Immunoblot of 8 mol/l urea-soluble fraction from the monkey spinal cord harvested 4 days (**B**) and 2 weeks (**C**) after onset of symptoms, using antibodies to pS409/410 TDP-43 (*top*) and C-TDP-43 (*bottom*) before (−) and after (+) treatment with lambda protein phosphatase (λPPase). 3 = Mixture of Flag-TDP-43- and TDP-43-expressing HEK 293T cell lysates. The phosphorylated TDP-43 was detected only in the late stage (asterisk).

necessary to initiate motor symptoms and is a late event in moto-neuron degeneration.

In the spinal cords of our monkeys, neither a C-terminal nor a phosphospecific TDP-43 antibody detected the 25-kDa C-terminal fragment that is found in patients with ALS. Overexpressed 25-kDa C-terminal fragment in cultured cells is reported to be toxic (Igaz et al., 2009; Zhang et al., 2009), and the accumulation of 25-kDa C-terminal fragment in transgenic mouse brain correlates with disease progression (Xu et al., 2010). Interestingly, unlike the FTLD/ALS brain, the 25-kDa C-terminal fragment is often absent in the ALS spinal cord (Neumann et al., 2009). The absence of 25-kDa C-terminal fragment in ALS spinal cord does not necessarily preclude a primary role for this form; rather it can be pathologically crucial if its absence is due to the accelerated degeneration of motoneurons with 25-kDa C-terminal fragment. It is difficult to deny that small amounts of C-terminal truncated species are actually present, because mislocalization of TDP-43 was focal in the spinal cord of our monkeys. However, the failure to detect 25-kDa C-terminal fragment in our monkey spinal cord at the early stage may have an implication that full-length TDP-43 is sufficient to be toxic, because α-motor axonal excitability was impaired but their cell bodies were preserved at autopsy.

The results of studies on the relationship between TDP-43 mislocalization and neuron loss remain controversial. The overexpression of wild-type TDP-43 in the nuclei in a transgenic rodent model was sufficient to be toxic to spinal motoneurons (Li et al., 2010; Shan et al., 2010; Wils et al., 2010; Xu et al., 2010), which is consistent with our observations in the rat model. In this context, it can be interpreted that the cytoplasmic mislocalization of wild-type TDP-43 is an epiphenomenon and not a necessary condition for the disease. However, in our monkey model, TDP-43 mislocalization was detected in almost all of the large motoneurons of the lateral nuclear group at the early or even the presymptomatic stage, and these motoneurons later showed neuron loss. In contrast, overexpressed exogenous TDP-43 in the large motoneurons of the ventromedial nuclear group was restricted to the nucleus, but did not produce neuron loss. Mice with over-expression of human TDP-43 engineered to localize in the cytoplasm showed progressive neuronal loss and downregulation of endogenous nuclear mouse TDP-43 expression (Igaz et al., 2011). These suggest that TDP-43 mislocalization is an upstream event in the cascade of motoneuronal degeneration. This finding is consistent with the observation that the highest percentage of neurons with TDP-43 mislocalization was found in the early stage of ALS in patients (Giordana et al., 2010).

In conclusion, our monkey model is superior to rodent models in recapitulating the TDP-43 pathology and in the presence of Bunina body-like inclusion and is expected to be a powerful tool for investigating developing effective therapies as well as the disease pathogenesis of sporadic ALS.

Acknowledgements

Funding

Supplementary material

Supplementary material is available at Brain online.

References

Anderson KD, Gunawan A, Steward O. Spinal pathways involved in the control of forelimb motor function in rats. Exp Neurol 2005; 194: 161–74.

Arai T, Hasegawa M, Akiyama H, Ikeda K, Nonaka T, Mori H, et al. TDP-43 is a component of ubiquitin-positive tau-negative inclusions in frontotemporal lobar degeneration and amyotrophic lateral sclerosis. Biochem Biophys Res Commun 2006; 351: 602–11.

Ash PE, Zhang YJ, Roberts CM, Saldi T, Hutter H, Buratti E, et al. Neurotoxic effects of TDP-43 overexpression in C. elegans. Hum Mol Genet 2010; 19: 3206–18.

Ayala YM, De Conti L, Avendaño-Vázquez SE, Dhir A, Romano M, D'Ambrogio A, et al. TDP-43 regulates its mRNA levels through a negative feedback loop. EMBO J 2011; 30: 277–88.

Bilsland LG, Sahai E, Kelly G, Golding M, Greensmith L, Schiavo G. Deficits in axonal transport precede ALS symptoms in vivo. Proc Natl Acad Sci USA 2010; 107: 20523–8.

Brooks BR, Miller RG, Swash M, Munsat TL. El Escorial revisited: revised criteria for the diagnosis of amyotrophic lateral sclerosis. Amyotroph Lateral Scler Other Motor Neuron Disord 2000; 1: 293–9.

Buratti E, Baralle FE. Characterization and functional implications of the RNA binding properties of nuclear factor TDP-43, a novel splicing regulator of CFTR exon 9. J Biol Chem 2001; 276: 36337–43.

Buratti E, Baralle FE. Multiple roles of TDP-43 in gene expression, splicing regulation, and human disease. Front Biosci 2008; 13: 867–8.

Buratti E, De Conti L, Stuani C, Romano M, Baralle M, Baralle F. Nuclear factor TDP-43 can affect selected microRNA levels. FEBS J 2010; 277: 2268–81.

Cairns NJ, Neumann M, Bigio EH, Holm IE, Troost D, Hatanpaa KJ, et al. TDP-43 in familial and sporadic frontotemporal lobar degeneration with ubiquitin inclusions. Am J Pathol 2007; 171: 227–40.

Carpenter MB, Sutin J. Human neuroanatomy. 8th edn. Baltimore: Williams & Wilkins; 1983.

Corbo M, Hays AP. Peripherin and neurofilament protein coexist in spinal spheroids of motor neuron disease. J Neuropathol Exp Neurol 1992; 51: 531–7.

De Carvalho M, Dengler R, Eisen A, England JD, Kaji R, Kimura J, et al. Electrodiagnostic criteria for diagnosis of ALS. Clin Neurophysiol 2008; 119: 497–503.

Dengler R, Konstanzer A, Küther G, Hesse S. Amyotrophic lateral sclerosis: Macro–EMG and twitch forces of single motor units. Muscle Nerve 1990; 13: 545–50.

Geser F, Lee VM, Trojanowski JQ. Amyotrophic lateral sclerosis and frontotemporal lobar degeneration: A spectrum of TDP-43 proteinopathies. Neuropathology 2010; 30: 103–12.

Giordana MT, Piccinini M, Grifoni S, De Marco G, Vercellino M, Magistrello M, et al. TDP-43 redistribution is an early event in sporadic amyotrophic lateral sclerosis. Brain Pathol 2010; 20: 351–60.

Gitcho MA, Bigio EH, Mishra M, Johnson N, Weintraub S, Mesulam M, et al. TARDBP 3′-UTR variant in autopsy-confirmed frontotemporal lobar degeneration with TDP-43 proteinopathy. Acta Neuropathol 2009; 11: 633–45.

Hanson KA, Kim SH, Wassarman DA, Tibbetts RS. Ubiquilin modifies TDP-43 toxicity in a Drosophila model of amyotrophic lateral sclerosis (ALS). J Biol Chem 2010; 285: 11068–72.

Harverkamp LJ, Appel V, Appel SH. Natural history of amyotrophic lateral sclerosis in a data base population. Validation of a scoring system and a model for survival prediction. Brain 1995; 118: 707–19.

Hasegawa M, Arai T, Nonaka T, Kametani F, Yoshida M, Hashizume Y, et al. Phosphorylated TDP-43 in frontotemporal lobar degeneration and amyotrophic lateral sclerosis. Ann Neurol 2008; 64: 60–70.

Igaz LM, Kwong LK, Chen-Plotkin A, Winton MJ, Unger TL, Xu Y, et al. Expression of TDP-43 C-terminal fragments in vitro recapitulates pathological features of TDP-43 proteinopathies. J Biol Chem 2009; 284: 8516–24.

Igaz LM, Kwong LK, Lee EB, Chen-Plotkin A, Swanson E, Unger T, et al. Dysregulation of the ALS-associated gene TDP-43 leads to neuronal death and degeneration in mice. J Clin Invest 2011; 121: 726–38.

Kabashi E, Lin L, Tradewell ML, Dion PA, Bercier V, Bourgouin P, et al. Gain and loss of function of ALS-related mutations of TARDBP (TDP-43) cause motor deficits in vivo. Hum Mol Genet 2010; 19: 671–83.

Kabashi E, Valdmanis PN, Dion P, Spiegelman D, McConkey BJ, Vande Velde C, et al. TARDBP mutations in individuals with sporadic and familial amyotrophic lateral sclerosis. Nat Genet 2008; 40: 572–4.

Körner S, Kollewe K, Fahlbusch M, Zapf A, Dengler R, Krampfl K, et al. Onset and spreading patterns of upper and lower motor neuron symptoms in amyotrophic lateral sclerosis. Muscle Nerve 2011; 43: 636–42.

Li Y, Ray P, Rao EJ, Shi C, Guo W, Chen X, et al. A Drosophila model for TDP-43 proteinopathy. Proc Natl Acad Sci USA 2010; 107: 3169–74.

Mackenzie IRA, Neumann M, Baborie A, Sampathu DM, Plessis DD, Jaros E, et al. A harmonized classification system for FTLD-TDP pathology. Acta Neuropathol 2011; 122: 111–3.

Mishra M, Paunesku T, Woloschak GE, Siddique T, Zhu LJ, Lin S, et al. Gene expression analysis of frontotemporal lobar degeneration of the motor neuron disease type with ubiquitinated inclusions. Acta Neuropathol 2007; 114: 81–94.

Mitsumoto H, Chad DA, Pioro EP. Amyotrophic lateral sclerosis. Philadelphia: F.A. Davis; 1998.

Munoz DG, Greene C, Perl DP, Selkoe DJ. Accumulation of phosphorylated neurofilaments in anterior horn motoneurons of amyotrophic lateral sclerosis patients. J Neuropathol Exp Neurol 1988; 47: 9–18.

Neumann M, Kwong LK, Lee EB, Kremmer E, Flatley A, Xu Y, et al. Phosphorylation of S409/410 of TDP-43 is a consistent feature in all sporadic and familial forms of TDP-43 proteinopathies. Acta Neuropathol 2009; 117: 137–49.

Neumann M, Sampathu DM, Kwong LK, Truax AC, Micsenyi MC, Chou TT, et al. Ubiquitinated TDP-43 in frontotemporal lobar degeneration and amyotrophic lateral sclerosis. Science 2006; 314: 130–3.

Okamoto K, Hirai S, Amari M, Watanabe M, Sakurai A. Bunina bodies in amyotrophic lateral sclerosis immunostained with rabbit anti-cystatin C serum. Neurosci Lett 1993; 162: 125–8.

Ou SH, Wu F, Harrich D, Garcia-Martinez LF, Gaynor RB. Cloning and characterization of a novel cellular protein, TDP-43, that binds to human immunodeficiency virus type 1 TAR DNA sequence motifs. J Virol 1995; 69: 3584–96.

Piao YS, Wakabayashi K, Kakita A, Yamada M, Hayashi S, Morita T, et al. Neuropathology with clinical correlations of sporadic amyotrophic lateral sclerosis:102 autopsy cases examined between 1962 and 2000. Brain Pathol 2003; 13: 10–22.

Polymenidou M, Lagier-Tourenne C, Hutt KR, Huelga SC, Moran J, Liang TY, et al. Long pre-mRNA deletion and RNA missplicing contribute to neuronal vulnerability from loss of TDP-43. Nat Neurosci 2011; 14: 459–68.

Pun S, Santos AF, Saxena S, Xu L, Caroni P. Selective vulnerability and pruning of phasic motoneuron axons in motoneuron disease alleviated by CNTF. Nat Neurosci 2006; 9: 408–19.

Shan X, Chiang PM, Price DL, Wong PC. Altered distributions of gemini of coiled bodies and mitochondria in motor neurons of TDP-43 transgenic mice. Proc Natl Acad Sci USA 2010; 107: 16325–30.

Swarup V, Phaneuf D, Bareil C, Robertson J, Rouleau GA, Kriz J, et al. Pathological hallmarks of amyotrophic lateral sclerosis/ frontotemporal lobar degeneration in transgenic mice produced with TDP-43 genomic fragments. Brain 2011; 134: 2610–26.

Tan CF, Eguchi H, Tagawa A, Onodera O, Iwasaki T, Tsujino A, et al. TDP-43 immunoreactivity in neuronal inclusions in familial amyotrophic lateral sclerosis with or without SOD1 gene mutation. Acta Neuropathol 2007; 113: 535–42.

Tateishi T, Hokonohara T, Yamasaki R, Miura S, Kikuchi H, Iwaki A, et al. Multiple system degeneration with basophilic inclusions in Japanese ALS patients with FUS mutation. Acta Neuropathol 2010; 119: 355–64.

Voigt A, Herholz D, Fiesel FC, Kaur K, Müller D, Karsten P, et al. TDP-43-mediated neuron loss in vivo requires RNA-binding activity. PLoS ONE 2010; 5: e12247.

Wils H, Kleinberger G, Janssens J, Pereson S, Joris G, Cuijt I, et al. TDP-43 transgenic mice develop spastic paralysis and neuronal inclusions characteristic of ALS and frontotemporal lobar degeneration. Proc Natl Acad Sci USA 2010; 107: 3858–63.

Xu YF, Gendron TF, Zhang YJ, Lin WL, D'Alton S, Sheng H, et al. Wild-type human TDP-43 expression causes TDP-43 phosphorylation, mitochondrial aggregation, motor deficits, and early mortality in transgenic mice. J Neurosci 2010; 30: 10851–9.

Yokoseki A, Shiga A, Tan CF, Tagawa A, Kaneko H, Koyama A, et al. TDP-43 mutation in familial amyotrophic lateral sclerosis. Ann Neurol 2008; 63: 538–42.

Zhang YJ, Xu YF, Cook C, Gendron TF, Roettges P, Link CD, et al. Aberrant cleavage of TDP-43 enhances aggregation and cellular toxicity. Proc Natl Acad Sci USA 2009; 106: 7607–12.

Original Article

Neuropathologic analysis of Lewy-related α-synucleinopathy in olfactory mucosa

Sayaka Funabe,[1,4] Masaki Takao,[1] Yuko Saito,[5] Hiroyuki Hatsuta,[1] Mikiko Sugiyama,[1] Shinji Ito,[1] Kazutomi Kanemaru,[2] Motoji Sawabe,[3] Tomio Arai,[3] Hideki Mochizuki,[6] Nobutaka Hattori[4] and Shigeo Murayama[1]

Departments of [1]Neuropathology, [2]Neurology, [3]Pathology, Tokyo Metropolitan Geriatric Hospital and Institute of Gerontology, [4]Department of Neurology, Juntendo University, [5]Department of Laboratory Medicine, National Center Hospital for Neurology and Psychiatry, Tokyo and [6]Department of Neurology, Faculty of Medicine, Osaka University, Osaka, Japan

We analyzed the incidence and extent of Lewy-related α-synucleinopathy (LBAS) in the olfactory mucosa, as well as the central and peripheral nervous systems of consecutive autopsy cases from a general geriatric hospital. The brain and olfactory mucosa were immunohistochemically examined using antibodies raised against phosphorylated α-synuclein. Thirty-nine out of 105 patients (37.1%) showed LBAS in the central or peripheral nervous systems. Seven patients presented LBAS (Lewy neurites) in the olfactory lamina propria mucosa. One out of the seven cases also showed a Lewy neurite in a bundle of axons in the cribriform plate, but α-synuclein deposits were not detected in the olfactory receptor neurons. In particular, high incidence of α-synuclein immunopositive LBAS in the olfactory mucosa was present in the individuals with clinically as well as neuropathologically confirmed Parkinson's disease and dementia with Lewy bodies (6/8 cases, 75%). However, this pathologic alteration was rare in the cases with incidental or subclinical Lewy body diseases (LBD) (one out of 31 cases, 3.2%). In the olfactory bulb, the LBAS was usually present in the glomeruli and granular cells of most symptomatic and asymptomatic cases with LBD. Our studies further confirmed importance of the olfactory entry zone in propagation of LBAS in the human aging nervous system.

Key words: α-synuclein, Lewy body, neuropathology, olfactory mucosa, Parkinson's disease.

INTRODUCTION

Sporadic Parkinson's disease is a neurodegenerative disorder characterized clinically by resting tremor, rigidity, bradykinesia and gait disturbance, as well as neuropathologically by the loss of neurons in several brainstem nuclei and the presence of Lewy bodies formed by abnormal accumulation of α-synuclein.[1-5] Of the many types of neurons in the central and peripheral nervous systems, a specific subset of neurons is vulnerable to accumulation of α-synuclein, which takes the form of aggregates such as Lewy bodies and Lewy neurites (LBs/LNs).[6-8]

Based on studies of a large number of autopsy cases, the initial sites involved in Lewy-related pathology are reported to be the dorsal motor nucleus of the vagus, the intermediate reticular zone in the lower brainstem and olfactory bulb.[9,10] We previously reported that in the earliest stage of Lewy-related α-synucleinopathy (LBAS), abnormal α-synuclein accumulation extends from the peripheral part of the olfactory bulb to the anterior olfactory nucleus as well as the amygdala.[11] From a clinical standpoint, impaired olfactory function constitutes one of the earliest symptoms of sporadic Parkinson's disease.[12,13] Therefore, the olfactory system may be one of the vital regions in the development of Lewy body disease (LBD).

In the olfactory bulb, α-synuclein accumulation is observed in the anterior olfactory nucleus as well as the mitral, tufted, and granular cells of individuals with clinical Parkinson's disease or dementia with Lewy bodies (DLB). Even in the early stages of these diseases, LNs, LBs or both, can be seen in the olfactory bulbs.[11,14,15] Based on the results of a neuropathologic study, Beach et al. suggested that the olfactory bulb may be a candidate region of biopsy study to

confirm the diagnosis of LBD.[16] However, the biopsy of olfactory bulb is too invasive and difficult to carry out for patients without risk.[17,18]

The olfactory epithelium is composed of paraneurons and neurites from which the glomeruli of the olfactory bulb originate. However, a neuropathologic analysis of LBAS has not been carried out adequately for LBD. Duda *et al.* reported that normal α-synuclein is expressed in the basal cells, olfactory receptor neurons, supporting cells, and Bowman's glands of the olfactory epithelium in normal controls, as well as patients with Parkinson's disease, Alzheimer disease and multiple system atrophy.[19] However, pathologic α-synuclein accumulation is rare (3.7%) among both normal controls and individuals affected by DLB, Alzheimer disease or Parkinson's disease.[20] According to a biopsy study of the olfactory epithelium in individuals with Parkinson's disease and younger hyposmic controls, no specific pathologic alteration was found.[21]

Therefore, it is still controversial whether abnormal α-synuclein accumulation in the olfactory epithelium precedes the formation of LBs/LNs in the olfactory bulb and contributes to olfactory dysfunction in sporadic Parkinson's disease. The aim of this study was to clarify the neuropathologic alterations of the olfactory mucosa in LBD by immunohistochemical analysis of a series of autopsied individuals.

MATERIALS AND METHODS

Tissue source

Tissue samples were obtained from autopsy materials that were collected at the Tokyo Metropolitan Geriatric Hospital and Institute of Gerontology between October 2008 and August 2010. This hospital is located at the center of Tokyo city and is a geriatric general emergency hospital with 579 beds. This hospital provides community-based medical service to the aged population 24 h/day in cooperation with local general practitioners. The number of autopsy cases was 162 in the above duration. In addition to the general organs, we could obtain the brains and spinal cords from 105 cases in that period, that were registered to the Brain Bank for Aging Research (BBAR) with the deceased's relatives' informed consent. The BBAR is approved by the ethics committee of the Tokyo Metropolitan Geriatric Hospital and Institute of Gerontology to carry out comprehensive research.

Clinical information

All clinical information, including the presence or absence of Parkinsonism as well as dementia, was retrospectively

obtained from medical charts and reviewed by two board-certified neurologists.[11,22–26] First, we evaluated Parkinsonism such as bradykinesia, resting tremor, rigidity and postural instability. In this study, when individuals had two or more of these four clinical symptoms, we defined them as having Parkinson's disease-related symptoms.[27] Second, we analyzed scores for the Mini-Mental State Examination[28] or the Hasegawa Dementia Scale (or its revised version),[29,30] the Instrumental Activities of Daily Living,[31] and the Clinical Dementia Rating (CDR).[32] When individuals were not assigned to a category of CDR, we retrospectively determined CDR using medical records, including the battery of cognitive tests above, as well as interviews with attending physicians and caregivers when necessary. Based on these results, we assigned a clinical diagnosis to each patient. The clinical diagnosis of Alzheimer disease was carried out based on the criteria of the National Institute of Neurological and Communication Disorders and Stroke-Alzheimer Disease and Related Disorders Association.[33] The diagnosis of DLB and Parkinson's disease with dementia conformed to the third report of the DLB consortium.[34]

Histology

We examined the brain and olfactory epithelium, olfactory bulb, esophagogastric mucosal junction, sympathetic ganglia, thoracic spinal cord, adrenal glands, anterior wall of the left ventricle of the heart, and abdominal skin.[22,26] The brains and spinal cords were examined as previously reported.[22,24,25] Briefly, the cerebral and cerebellar hemispheres as well as brainstem were dissected in the sagittal plane at the time of autopsy. In each case, half of the brain was preserved at −80°C for further biochemical and molecular analyses. The other half of the brain and abdominal skin were fixed in 20% buffered formalin (WAKO, Osaka, Japan) for 7–13 days and sliced in the same manner as the contralateral hemisphere. The adrenal gland and anterior wall of the left ventricle of the heart were fixed in 20% formalin. The representative areas were embedded in paraffin. Six-micrometer-thick serial sections were cut and stained with HE and KB. Sections of the amygdala, hippocampus, parahippocampal gyrus and temporal cortex were stained with the modified Gallyas-Braak method for senile plaques, NFTs and argyrophilic grains.[35]

Immunohistochemistry

Sections were immunostained using the following antibodies raised against phosphorylated tau protein (p-tau) (AT8, monoclonal; Innogenetics, Temse, Belgium): synthetic peptide corresponding to amino acids 11–28 of amyloid-beta protein (12B2, monoclonal; IBL, Maebashi, Japan); phosphorylated α-synuclein (pSyn#64, monoclonal[25] and

Table 1 Antibodies used for immunohistochemistry

Antibody	Epitope	Source	Clone	Dilution ratio	Antigen method	Retrieval (min)
pSyn#64	α-synuclein phosphorylated ser 129	T. Iwatsubo	Monoclonal	1:20000	99% formic acid	5
PSer129	α-synuclein phosphorylated ser 129	T. Iwatsubo	Polyclonal	1:100	None	
PGP9.5	PGP9.5	Biomol	Polyclonal	1:5000	microwave	30
SMI31	phosphorylated neurofilament	Sternberger	Monoclonal	1:20000	None	
Tyrosine hydroxylase	Anti-tyrosine hydroxylase, rat	CALBIOCHEM	Monoclonal	1:10	microwave	30
AT8	Phosphorylated tau protein	Innogenetics	Monoclonal	1:1000	None	
12B2	Aβ11–28	IBL	Monoclonal	1:50	99% formic acid	5

PSer129 polyclonal[36]), ubiquitin (polyclonal, Sigma-Aldrich, St. Louis, MO), Protein Gene Product 9.5 (PGP9.5, polyclonal; ENZO Life Sciences International, Farmingdale, NY USA); phosphorylated neurofilament (SMI31, monoclonal; Sternberger Immunochemicals, Bethesda, MA, USA); and tyrosine hydroxylase (Anti-Tyrosine Hydroxylase, Rat, monoclonal; Calbiochem-Novabiochem Corporation, Darmstadt, Germany) (Table 1). The signals from monoclonal and polyclonal antibodies were detected by using the automatic system on a VENTANA NX20 with the I-View DAB Universal Kit (Roche, Basel, Switzerland) according to the manufacturer's instructions. Sections were counter-stained with hematoxylin.

LBAS

CNS

In order to analyze LBAS,[22] we carried out immunohistochemical analysis with phosphorylated α-synuclein antibodies for the following sections: the medulla oblongata at the level of the dorsal motor nucleus of the vagus, the upper pons at the level of the locus coeruleus, and the midbrain including the substantia nigra, amygdala, anterior hippocampus and the peripheral nervous system from all cases (described in the next section). When immunopositive deposits were observed in these anatomic regions, we carried out additional immunohistochemical analysis for sections of the basal nucleus of Meynert, anterior cingulate gyrus, entorhinal cortex, the second frontal and temporal gyri and the supramarginal gyrus, using antibodies raised against phosphorylated α-synuclein.

Peripheral nervous system

To analyze LBAS of the peripheral nerve, tissue sections from epicardium and epicardial fat of the left ventricle of the heart, sympathetic ganglia, esophagogastric mucosal junction, adrenal gland[22] and abdominal skin[26] were examined by using antibodies raised against phosphorylated α-synuclein.

© 2012 Japanese Society of Neuropathology
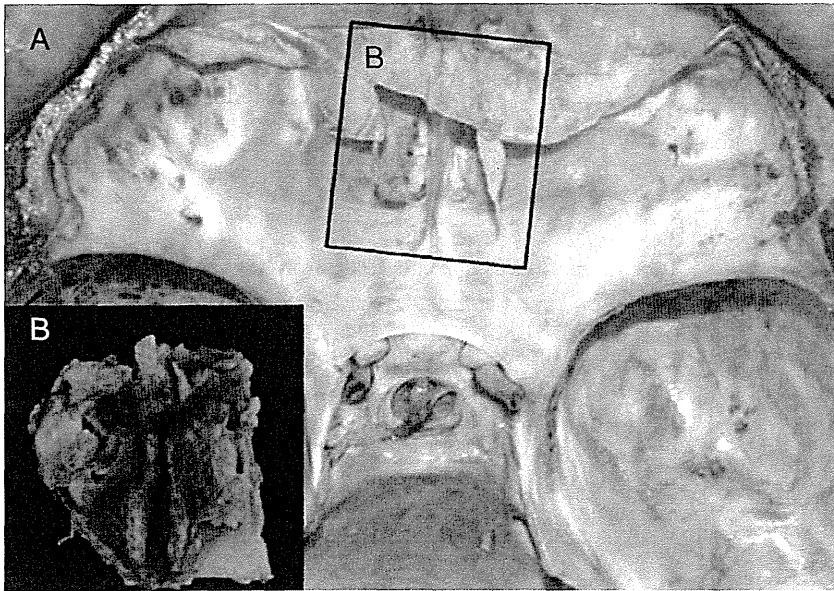
Olfactory mucosa

At the time of autopsy, the olfactory mucosa, bony septae and contiguous cribriform plate were removed en bloc (Fig. 1). The cribriform plate was dissected in the sagittal plane of the midline by using an electric jigsaw. The left side was fixed for 24 h in 4% paraformaldehyde. After fixation, the olfactory mucosa was removed, dehydrated in a graded alcohol series, cleared in xylene and embedded in paraffin. The right side was fixed for 24 h in 4% paraformaldehyde, decalcified with EDTA for 2 weeks, and dehydrated and embedded in paraffin. Serial 6-μm-thick sections were stained with HE and immunolabeled with antibodies against phosphorylated α-synuclein, PGP9.5, phosphorylated neurofilament, tyrosine hydroxylase, phosphorylated tau and amyloid β (Table 1). In particular, the olfactory receptor neurons of the olfactory epithelium were identified by using PGP9.5 immunohistochemistry.[19] The normal anatomical appearance of the olfactory system is shown in Figure 2.

Olfactory bulb

The olfactory bulbs were prepared for histologic sections to analyze the presence of LBAS. By using HE stain and α-synuclein antibodies, LBAS were identified in the glomeruli, mitral cells, tufted cells and granular cells as previously reported.[11] Mitral and tufted cells were distinguished by their specific shapes. Each neuron was identified when it had an apparent nucleus containing a prominent nucleolus and Nissl substance.

Semiquantitative scoring system of Lewy-related pathology

For each section, we semi-quantitatively graded the immunohistochemical staining with antibody raised against phosphorylated α-synuclein. Our grading system was modified based on the scoring system of the third report of the DLB consortium[34] because we used both the HE stain and immunohistochemistry using monoclonal antibody for phosphorylated α-synuclein to identify LBAS.

Fig. 1 (a) The anterior cranial fossa after removal of the brain. In order to obtain the olfactory mucosa, the bony septae and contiguous cribriform plate (the rectangular area) were dissected using an electric jigsaw. (b) An inset shows the olfactory mucosa and cribriform plate from the opposite side of the rectangular area.
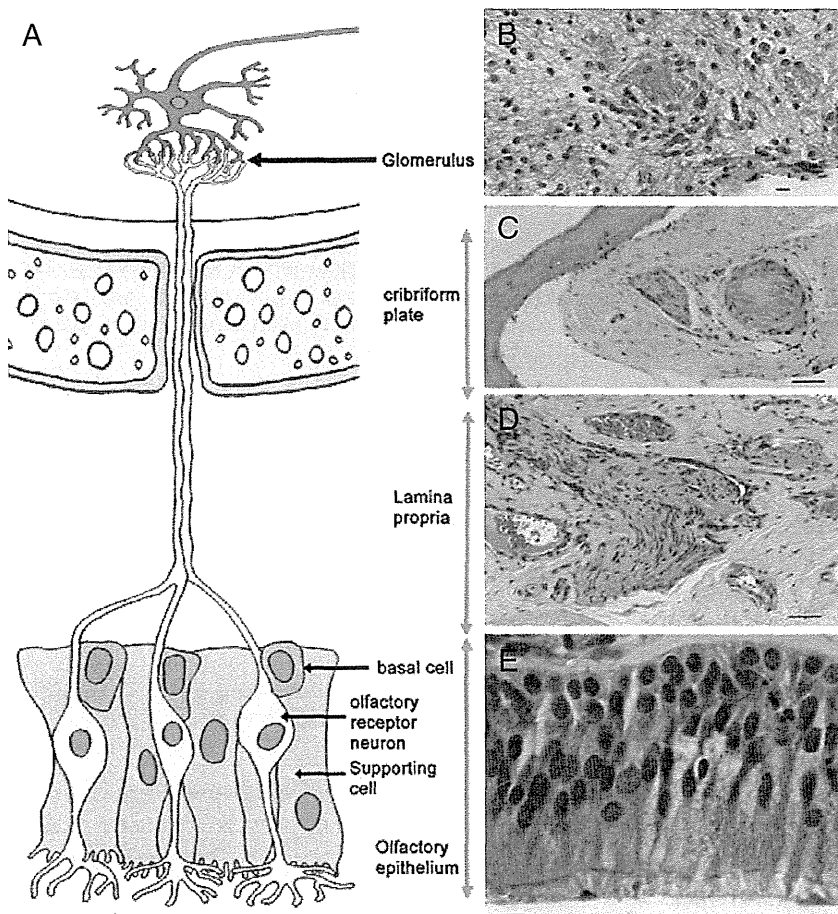
Fig. 2 Scheme of the normal olfactory pathway (a) and photomicrographs of representative histologies of each region (b–e). The olfactory epithelium is composed of three cell types: the basal cells, olfactory receptor neurons and supporting cells (a). The basal cells are the progenitor of the olfactory receptor neurons (a, e). In general, the turnover rate of the olfactory receptor neurons is approximately 30–90 days. Nerve fibers are present in the lamina propria and cribriform plate (c and d, respectively). They consist of either the axons of the olfactory receptor neurons or postganglionic sympathetic nerve fibers. There are glomeruli in the olfactory bulb (b). Glomeruli are the synaptically connected structures of the axons of the olfactory receptor neurons and mitral/tufted cells in the olfactory bulb. (b, e), scale bar = 10 μm; (c), scale bar = 50 μm; (d), scale bar = 100 μm.

For example, 'Stage 1' of the original scoring system was defined as 'sparse Lewy bodies or neurites.' On the other hand, 'Grade 1'of our methodology is defined as 'sparse Lewy neurites without Lewy bodies.'

Grade 0 = neither LNs nor LBs detected using anti-phosphorylated α-synuclein antibody.

Grade 1 = sparse phosphorylated α-synuclein immunopositive dots or neurites, or diffuse granular cytoplasmic stain in the neuron, neither LBs nor phosphorylated α-synuclein-immunopositive neuronal intracytoplasmic dense aggregations.

Grade 2 = 1–3 LBs or phosphorylated α-synuclein-immunopositive intracytoplasmic dense aggregations and scattered LNs in a low-power field (×10).

Grade 3 = more than four LBs and scattered LNs in a low-power field (×10).

Grade 4 = numerous LBs and neurites with severe immunoreactivity for phosphorylated α-synuclein in the neuropil or background.

LB staging system of our BBAR (BBAR LB stage)

In order to assess the clinical and neuropathologic alterations of LBD, we applied the following rating system to our BBAR for all autopsy cases (Table 2, Fig. 3). The original BBAR LB staging system was developed in order to track the individual data of our brain bank.[24,25] This rating system requires clinical symptoms, gross and microscopic neuropathologic alterations, and LB scores used in the consensus guidelines for the clinical and pathologic diagnosis of DLB.[27] In this staging system, Parkinson's disease with

Table 2 Lewey body stage of Brain Bank for Aging Research

Stage	Psyn-IR	LB	SN: loss of pigmentation	LB score	Dementia	Parkinsonism	Diagnosis
0	−	−	−				
0.5	+	−	−				
1	+	+	−				Incidental LBD
2	+	+	+	0–10	−†	−†	Subclinical LBD
3	+	+	+	0–10	−	+	PD
4	+	+	+	3–6	+	+	PDDL
	+	+	+	3–6	+	+ or −	DLBL‡
5	+	+	+	7–10	+	+	PDDN
	+	+	+	7–10	+	+ or −	DLBN‡

†Neither dementia nor Parkinsonism associated with Lewy body-related α-synucleinopathy. ‡Differential diagnosis of PDD and DLB was based on the '1-year rule' according to the consensus guidelines (34). DLBL, dementia with Lewy bodies and a Lewy body score corresponding to the limbic form; DLBN, dementia with Lewy bodies and a Lewy body score corresponding to the neocortical form; LB, Lewy body; LBD, Lewy body disease; PD, Parkinson's disease; PDDL, Parkinson's disease with dementia and a Lewy body score corresponding to the limbic form; PDDN, Parkinson's disease with dementia and a Lewy body score corresponding to the neocortical form; Psyn-IR, phosphorylated alpha-synuclein immunoreactivity; SN, substantia nigra.
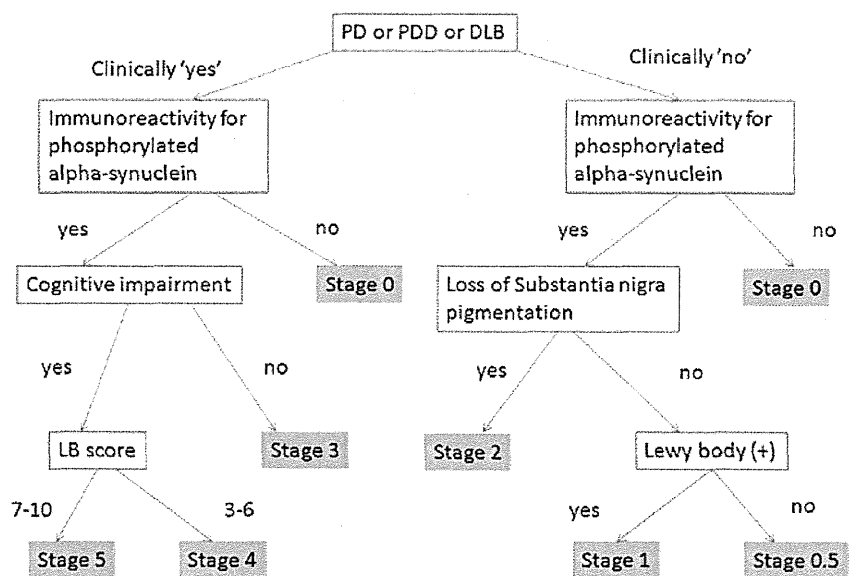
Fig. 3 Flow-chart of the Lewy body staging system of the Brain Bank for Aging Research (BBAR). PD, Parkinson's disease; PDD, Parkinson's disease with dementia; DLB, dementia with Lewy bodies; SN, substantia nigra; LB score, Lewy body score. See Table 2 for detailed description of each stage.

© 2012 Japanese Society of Neuropathology

dementia was differentiated from DLB by applying the '12-month (1-year)' rule noted in the Consensus Guidelines (i.e., 'dementia appears more than one year after the onset of Parkinsonism').[27]

Evaluation of senile changes and neuropathologic diagnosis

NFTs were classified according to Braak and Braak's staging system using modified Gallyas-Braak staining[37] and AT8 immunohistochemistry.[38] The staging system for senile plaques (SPs) comprises four stages (0–C). Argyrophilic grains were classified into our four stages (0–III), as reported previously.[23] The neuropathologic diagnosis of Alzheimer disease was based on our previous definition,[39] which proposed a modification of the National Institute on Aging and Reagan Institute criteria.[40,41] The diagnoses of dementia with grains and NFT-predominant forms of dementia were based on the previously described definitions.[42,43]

Statistical analysis

Fisher's exact test was carried out to compare the number of cases having LBAS pathology in the olfactory mucosa.

RESULTS

Clinical information

Of the 105 consecutive autopsy patients, 58 were men and 47 were women. The patient ages at death ranged from 65 to 104 years (82 ± 37, mean ± SD). Twelve patients showed Parkinson's disease-related symptoms according to the clinical criteria in this study. Six out of 105 patients were clinically diagnosed as LBD including Parkinson's disease, Parkinson's disease with dementia and DLB.

Neuropathologic diagnosis

The neuropathologic diagnoses consisted of Alzheimer disease ($n = 15$), dementia with grains ($n = 11$), NFT-predominant form of dementia ($n = 8$), Parkinson's disease ($n = 2$), Parkinson's disease with dementia ($n = 2$), and DLB ($n = 1$), as well as one case each of dentatorubral-pallidoluysian atrophy, neuronal hyaline inclusion body disease, frontotemporal lobar degeneration with transaction response (TAR) DNA-binding protein-43 kDa-immunoreactive inclusions, and progressive multifocal leukoencephalopathy. Patients with combined pathologies, included Alzheimer's disease plus DLB ($n = 2$), dementia with grains plus NFT-predominant form of dementia ($n = 3$), and one patient each of diffuse NFTs with calcification (DNTC)[44] plus DLB and dementia with grains plus

Alzheimer's disease. The remaining patients did not fulfil the clinical and/or pathological criteria for neurodegenerative diseases.

Eight out of 105 patients (8/105 = 7.6%) were clinically and neuropathologically diagnosed as having LBD, including Parkinson's disease (2 patients), Parkinson's disease with dementia (2 patients) and DLB (4 patients).

Incidence, distribution and extent of LBAS

BBAR staging

Based on clinical and neuropathologic analyses, the BBAR LB stages were as follows: stage 0 = 66 cases, stage 0.5 = 6 cases, stage 1 = 21 cases, stage 2 = 4 cases, stage 3 = 2 cases, stage 4 = 3 cases and stage 5 = 3 cases. All of the stage 5 cases had DLB, with an LB score corresponding to the value for the neocortical form (DLBN).

LBAS in CNS and peripheral nervous system

We identified 39 (37.1%) out of the 105 individuals with α-synuclein immunopositive LBAS in the CNS or peripheral nervous system (Table 3). Therefore, we focused on these 39 cases in the present study. Here, LBAS was identified by using α-synuclein immunohistochemistry. In LBAS, LBs were confirmed with HE stains and α-synuclein immunohistochemistry. Out of the 39 cases, 33 showed LBAS in the olfactory bulb, 15 in the enteric nerve plexus, 23 in the sympathetic ganglia, and 16 in the pericardial nerve fibers of the left ventricle (Tables 3 and 4).

Olfactory mucosa

The olfactory epithelium is a pseudostratified columnar epithelium lying deep within the recess of the superior nasal cavity; it is composed of a mixture of multipotential stem cells (basal cells), supporting cells and olfactory receptor neurons (Fig. 2). Mature neurons are reported to give rise to fine and unmyelinated axons that ascend through the cribriform plate to synapse at glomeruli in the olfactory bulb.[20,45]

LBAS were found in the olfactory mucosa of seven (17.9%) out of 39 cases (Tables 3 and 4). These seven also had LBAS in the olfactory bulb. LBAS was present in the lamina propria mucosa of the seven cases (Fig. 4a–c). In addition, one case showed LBAS in a bundle of axons in the cribriform plate (Fig. 4d). None of the cases showed LBAS in the olfactory epithelial paraneuron. We summarized the demographic results of these seven individuals with LBAS in the olfactory mucosa in Table 5. Neither phosphorylated tau-positive deposits nor amyloid β immunopositive deposits were detected in the olfactory mucosa.

**Table 3** The distribution of α-synuclein deposits in various anatomical regions of 39 cases with Lewy body disease

Age at death/gender	Parietal lobe	Frontal lobe	Temporal lobe	Cingulate gyrus	Entorhinal cortex	Amygdala	Olfactory bulb	Nucleus basalis of Meynert	Substantia nigra	Locus coeruleus	Dorsal motor nucleus of the vagus	Spinal Cord	Gastrointestinal system	Olfactory Mucosa	Sympathetic ganglion	Adrenal gland	Pericardial nerve	Skin	BBAR LB stage	NFT stage	SP stage
104/F																			5	4	C
70/F																			5	4	C
86/F																			5	6	C
84/M																			4	2	A
79/F																			4	2	A
80/F																			4	2	A
81/M																			3	2	A
88/M																			3	3	A
79/M																			2	1	A
68/F																			2	2	B
79/F																			2	6	C
77/F																			2	6	C
78/M																			1	2	A
75/M																			1	2	A
89/F																			1	3	C
93/F																			1	4	C
86/M																			1	4	C
81/M																			1	2	A
90/F																			1	2	A
86/M																			1	2	A
97/F																			1	2	A
78/M																			1	1	A
92/M																			1	3	C
94/M																			1	4	A
85/M																			1	3	A
81/F																			1	5	C
96/F																			1	2	0
87/F																			1	3	A
101/F																			1	4	A
69/F																			1	4	0
83/F																			1	3	A
72/M																			1	1	A
77/M																			1	2	A
83/M																			0.5	4	C
71/M																			0.5	2	A
89/M																			0.5	2	A
85/F																			0.5	3	A
85/F																			0.5	2	A
96/F																			0.5	3	A

Grade 0 = blank, grade 1 = light grey, grade 2 = light blue, grade 3 = blue, grade4 = navy blue. The number in each cell indicates a score based on the semiquantitative scoring system of Lewy-related pathology. 0 = neither Lewy neurites nor bodies detected by using anti-phosphorylated α-synuclein antibody. 1 = sparse phosphorylated α-synuclein immunopositive dots or neurites, neither Lewy bodies nor phosphorylated α-synuclein immunopositive intracytoplasmic aggregations. 2 = one to three Lewy bodies or phosphorylated α-synuclein immunopositive intracytoplasmic aggregations in a low-power field (×10). 3 = more than four Lewy bodies and scattered Lewy neurites in a low-power field (×10). 4 = numerous LBs and neurites with severe immunoreactivity for phosphorylated α-synuclein in the neuropil or background. Individuals of BBAR LB stages 3–5, with clinical Parkinsonism and neuropathologically numerous LBASs in the CNS, showed high incidence (75%, 6/8 individuals) of LBASs in the olfactory mucosa. In contrast, individuals of BBAR LB stages 1–3 without Parkinsonism showed extremely low incidence of Lewy body-related α-synucleinopathy (LBAS) (3%, 1/31) in the olfactory mucosa. LBAS was found in the olfactory mucosa mostly in advanced BBAR LB stages 3–5. BBAR LB Brain Bank for Aging Research Lewy body staging, NFT stage, Braak's stages for neurofibrillary tangles; SP stage, Braak's stages for senile plaques.

© 2012 Japanese Society of Neuropathology

Table 4 Regional frequency of Lewy body-related α-synucleinopathy (LBAS) in various anatomical regions

The BBAR LB stage	Olfactory epithelium	Olfactory mucosa	Olfactory bulb	Spinal cord	GI tract	Sympathetic ganglia	Adrenal gland	Pericardial nerve	Skin
0.5	0/6	0/6	2/6	0/6	0/6	2/6	0/6	1/6	0/6
1	0/21	1/21	19/21	7/21	6/27	10/21	1/21	6/21	1/21
2 ·	0/4	0/4	4/4	3/4	1/4·	3/4	0/4	2/4	0/4
3	0/2	1/2	2/2	2/2	2/2	2/2	2/2	1/2	2/2
4	0/3	3/3	3/3	3/3	3/3	3/3	3/3	3/3	2/3
5	0/3	2/3	3/3	3/3	3/3	3/3	1/3	3/3	0/3
All	**0/39**	**7/39**	**33/39**	**18/39**	**15/39**	**23/39**	**7/39**	**16/39**	**5/39**

BBAR LB Brain Bank for Aging Research Lewy body staging.
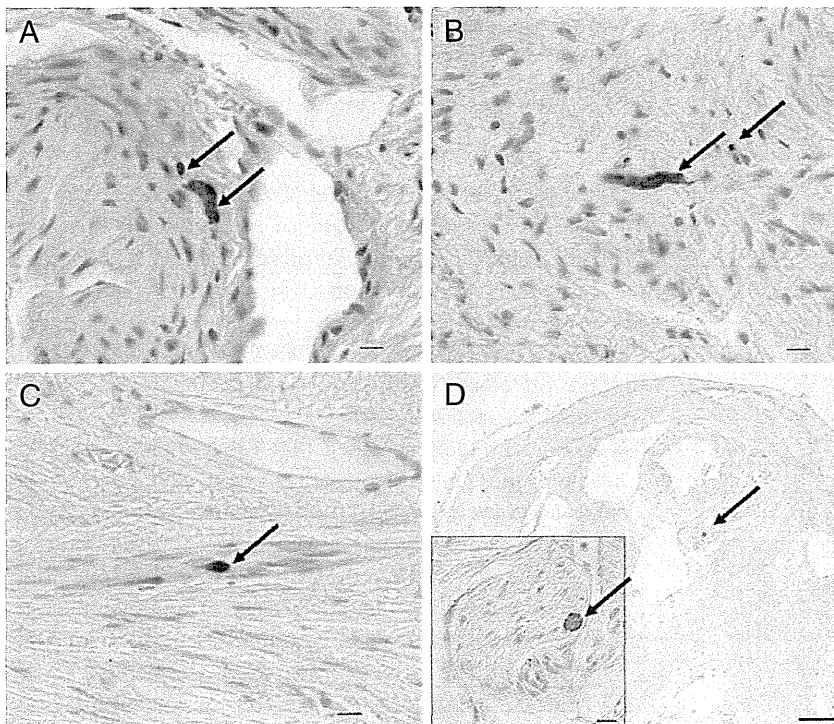
Fig. 4 Photomicrographs show α-synuclein immunopositive deposits (arrows indicate Lewy neurites) in the axonal bundle of the lamina propria (a–c) and cribriform plate (d). The inset in figure (d) shows a higher magnification image of α-synuclein immunopositive deposits in the axonal bundle of the cribriform plate. Immunohistochemistry using monoclonal antibody against phosphorylated α-synuclein (pSyn#64). Photomicrographs (a, b, c and d) were obtained from cases 4, 5, 7 and 3, respectively, in Table 5. (a–c), scale bar = 10 μm; (d) scale bar = 100 μm (inset, 10 μm).

Correlations between α-synuclein immunopositive LBs or LNs in the olfactory mucosa and CNS

Alpha-synuclein immunopositive LBs or LNs in the olfactory mucosa were detected in seven cases, including three with DLB, three with Parkinson's disease or Parkinson's disease with dementia, and one with incidental LBD (Tables 3–5). LBAS in the olfactory mucosa was compared with those in other locations of the CNS (Table 3). Individuals of BBAR LB stages 3–5, clinical and neuropathological diagnosis of LBD, showed a high incidence (75%, 6/8 individuals) of α-synuclein immunopositive LBAS in the olfactory mucosa (Table 6, Fig. 5). Six individuals with Parkinson's disease also showed a high incidence of α-synuclein accumulation (66%, 4/6 individuals) in the olfactory mucosa. In contrast, individuals of BBAR LB

stages 0.5–2 (here we classified them into asymptomatic group) showed a low incidence of LBAS (3%, 1/31) in the olfactory mucosa.

Olfactory bulb

There is neural connectivity among olfactory receptor neurons and nuclei in the olfactory bulbs.[45] Hence, we analyzed the frequency of LBAS in the glomeruli, tufted cells, mitral cells and granular cells between LBAS-positive and LBAS-negative groups in the olfactory epithelium.

In individuals of BBAR LB stages 3–5 (symptomatic stage), LBAS was frequently observed in the glomeruli (8/8 cases, 100%), granular cells (8/8, 100%) and tufted cells (7/8, 87.5%). In contrast, there were low numbers of cases with LBAS in the mitral cells (2/8, 25%). Asymptomatic stage cases of LBD, corresponding to BBAR stage 0.5–2,

Table 5 Clinical and neuropathological demography of seven individuals with Lewy body-related α-synucleinopathy (LBAS) identified in the olfactory mucosa

No.	Age at death	Clinically diagnosed as LBD	Cause of death	Neuropathologic diagnosis	BBAR LB stage	LBAS in the olfactory mucosa			NFT stage	SP stage
						Olfactory epithelium	Lamina propria mucosa	Cribriform plate		
1	104/F	None	CHF, MI, Dementia	DLBN, AD	5	0	1	0	1	C
2	70/F	DLB	DLB, pneumonia	DLBN, AD	5	0	1	0	1	C
3	84/M	DLB	Prostate carcinoma, DLB	DLBL	4	0	1	1	2	A
4	79/F	PDD	PDD	PDDN	4	0	1	0	2	A
5	80/F	PD	Pneumonia, PD	PDDL	4	0	1	0	2	A
6	88/M	PD	Pneumonia, PD	PD	3	0	1	0	2	A
7	86/M	None	Pneumonia	AD, Incidental LBD	1	0	1	0	1	C

AD, Alzheimer's disease; BBAR LB stage, Lewy body staging system of the Brain Bank for Aging Research; CHF, congestive heart failure; DLB, dementia with Lewy bodies; DLBL, dementia with Lewy bodies and a Lewy body score corresponding to the limbic form; DLBN, dementia with Lewy bodies and a Lewy body score corresponding to the neocortical form; F, female; LB, Lewy body; LBD, Lewy body disease; M, male; MI, acute myocardial infarction; NFT stage, Braak's stages for neurofibrillary tangles; PD, Parkinson's disease; PDDL, Parkinson's disease with dementia and a Lewy body score corresponding to the limbic form; PDDN, Parkinson's disease with dementia and a Lewy body score corresponding to the neocortical form; SP stage, Braak's stages for senile plaques.

Table 6 Incidence of LBAS in the olfactory mucosa in cases with symptomatic LBD (BBAR stage 3–5)

Clinical and neuropathologic diagnosis of LBD	LBAS in OM		Total
	Present	Absent	
Symptomatic (BBAR 3–5)	6*	2	8
Asymptomatic (BBAR 0.5–2)	1	30	31

*$P < 0.05$. BBAR, Brain Bank for Aging Research; LBAS; Lewy body-related alpha-synucleinopathy; LBD, Lewey body disease; OM; olfactory mucosa.

showed high incidence of LBAS in the glomeruli (23/31, 74.1%) and granular cells (22/31, 70.9%) of the olfactory bulb (Fig. 5).
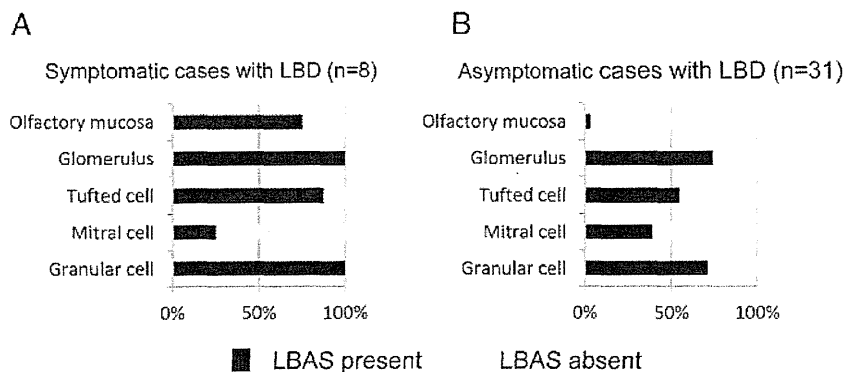
DISCUSSION

Our study provides two novel observations.

1 LBAS in the olfactory mucosa was frequently observed (6/8 cases, 75%) in the symptomatic patients with LBD, but was a rare condition (1/31 cases, 3.2%) in asymptomatic LBD patients.

2 LBAS was seen in the glomeruli and granular cells in the olfactory bulbs of most symptomatic and asymptomatic cases with LBD.

It has been widely accepted that LB pathology does not develop simultaneously in all anatomical regions of the central and peripheral nervous systems. Hawkes *et al.* proposed that neurotropic pathogens may enter the brain via two routes: (i) a nasal route, with anterograde progression into the temporal lobe; and (ii) a gastric route secondary to the swallowing of nasal secretions in saliva (a dual hit hypothesis).[46] The former route may be associated with the early accumulation of α-synuclein in the human olfactory bulb and cause olfactory dysfunction in sporadic Parkinson's disease. In the present study, there was rare observation of LBAS in the olfactory mucosa in the asymptomatic cases of LBD. Further analysis is important to clarify the possibility of propagation of α-synuclein in the nervous systems.

In the present study, LBAS was frequently observed in the olfactory mucosa (6/8 cases, 75%) in the individuals with clinical LBD. In contrast, LBAS in the olfactory mucosa was a rare observation in asymptomatic patients. It is also important that all seven cases with LBAS in the olfactory mucosa had LBAS in the cerebral cortex and brainstem. Our results have similarities with a previous report concerning Alzheimer's disease.[20] Detection of LBAS in the olfactory mucosa could be hindered by two problems: technical difficulty in obtaining enough nerve fibers and rapid turnover of olfactory receptor neurons.[47,48] In fact, a recent study reported that a biopsy study revealed no α-synuclein immunopositive deposits in the olfactory

A

Symptomatic cases with LBD (n=8)

B

Asymptomatic cases with LBD (n=31)

Fig. 5 Frequencies of cases having Lewy-related α-synucleinopathy (LBAS) pathology in the olfactory mucosa and each anatomical region of the olfactory bulb. (a) Cases with symptomatic dementia with Lewy bodies (LBD) (*n* = 8, Brain Bank for Aging Research [BBAR] stages 3–5). Most of the cases show LBAS pathology in the olfactory mucosa (6/8, 75%), glomeruli (8/8, 100%), tufted cells (6/7, 85.7%) and granular cells (8/8, 100%). The number of cases with LBAS in the mitral cells is low (2/6, 33.3%). (b) Cases with asymptomatic LBD (*n* = 25, BBAR stages 0.5–2). Most of the cases show LBAS pathology in the glomeruli (23/31, 74.1%), tufted cells (17/31, 54.8%) and granular cells (22/31, 70.9%). The number of cases with LBAS in the mitral cells (12/31, 38.7%) is low. LBAS pathology of the olfactory mucosa is present in only one case (1/31, 3.2%).

mucosa of patients of Parkinson's disease.[21] Our previous study indicated a high incidence of α-synuclein immunopositive LBs or neurites in aging human olfactory bulbs, and suggested that they extend from the periphery (the second olfactory structure) to the anterior olfactory nucleus (the tertiary olfactory structure).[11] The present study, using 6 μm-thick paraffin embedded sections, revealed that LBAS was most frequently observed in the glomeruli which were composed of axon terminals of olfactory epithelial cells and dendrites of mitral and tufted cells[45] as well as in the glomerular cells which were most numerous in the periphery of the olfactory bulb (Fig. 5). We consider that high incidence of LBAS in glomeruli may represent affected terminal axons of olfactory epithelial neurons. In contrast to our result, a previous study, employing 50 μm-thick floating sections, reported high frequency of LBAS in mitral cells and the internal plexiform layer in individuals with Parkinson's disease but no LBAS in age-matched controls.[49] Further studies are necessary to identify the most vulnerable subset in the periphery of the olfactory bulb.

In conclusion, presence of LBAS in the olfactory mucosa and olfactory glomeruli further supports the importance of olfactory system as an entry zone of LBD. Future studies of LB pathology involving the olfactory system are indicated to understand the pathomechanism of α-synuclein accumulation in individuals with LBD.

REFERENCES

1. Baba M, Nakajo S, Tu PH *et al*. Aggregation of alpha-synuclein in Lewy bodies of sporadic Parkinson's disease and dementia with Lewy bodies. *Am J Pathol* 1998; **152**: 879–884.
2. Spillantini MG, Crowther RA, Jakes R, Hasegawa M, Goedert M. alpha-Synuclein in filamentous inclusions of Lewy bodies from Parkinson's disease and dementia with Lewy bodies. *Proc Natl Acad Sci U S A* 1998; **95**: 6469–6473.
3. Goedert M, Spillantini MG, Davies SW. Filamentous nerve cell inclusions in neurodegenerative diseases. *Curr Opin Neurobiol* 1998; **8**: 619–632.
4. Ogunnyi A, Akang EE, Gureje O *et al*. Dementia with Lewy bodies in a Nigerian: a case report. *Int Psychogeriatr* 2002; **14**: 211–218.
5. Takao M, Ghetti B, Yoshida H *et al*. Early-onset dementia with Lewy bodies. *Brain Pathol* 2004; **14**: 137–147.
6. Braak H, Ghebremedhin E, Rub U, Bratzke H, Del Tredici K. Stages in the development of Parkinson's disease-related pathology. *Cell Tissue Res* 2004; **318**: 121–134.
7. Braak H, Sastre M, Bohl JR, de Vos RA, Del Tredici K. Parkinson's disease: lesions in dorsal horn layer I,

involvement of parasympathetic and sympathetic pre- and postganglionic neurons. *Acta Neuropathol* 2007; **113**: 421–429.

8. Braak H, Braak E. Pathoanatomy of Parkinson's disease. *J Neurol* 2000; **247** (Suppl 2): II3–I10.

9. Braak H, Del Tredici K, Rub U, de Vos RA, Jansen Steur EN, Braak E. Staging of brain pathology related to sporadic Parkinson's disease. *Neurobiol Aging* 2003; **24**: 197–211.

10. Del Tredici K, Rub U, De Vos RA, Bohl JR, Braak H. Where does Parkinson disease pathology begin in the brain? *J Neuropathol Exp Neurol* 2002; **61**: 413–426.

11. Sengoku R, Saito Y, Ikemura M *et al.* Incidence and extent of Lewy body-related alpha-synucleinopathy in aging human olfactory bulb. *J Neuropathol Exp Neurol* 2008; **67**: 1072–1083.

12. Ponsen MM, Stoffers D, Booij J, van Eck-Smit BL, Wolters ECh, Berendse HW. Idiopathic hyposmia as a preclinical sign of Parkinson's disease. *Ann Neurol* 2004; **56**: 173–181.

13. Haehner A, Boesveldt S, Berendse HW *et al.* Prevalence of smell loss in Parkinson's disease – a multicenter study. *Parkinsonism Relat Disord* 2009; **15**: 490–494.

14. Daniel SE, Hawkes CH. Preliminary diagnosis of Parkinson's disease by olfactory bulb pathology. *Lancet* 1992; **340** (8812): 186.

15. Pearce RK, Hawkes CH, Daniel SE. The anterior olfactory nucleus in Parkinson's disease. *Mov Disord* 1995; **10**: 283–287.

16. Beach TG, White CL 3rd, Hladik CL *et al.* Olfactory bulb alpha-synucleinopathy has high specificity and sensitivity for Lewy body disorders. *Acta Neuropathol* 2009; **117**: 169–174.

17. Parkkinen L, Silveira-Moriyama L, Holton JL, Lees AJ, Revesz T. Can olfacotry bulb biopsy be justified for the diagnosis of Parkinson's disease? Comments on 'olfactory bulb α-synucleinopathy has specificity and sensitivity for Lewy body disorders'. *Acta Neuropathol* 2009; **117** (2): 213–214.

18. Jellinger KA. Olfactory bulb α-synucleinopathy has specificity and sensitivity for Lewy body disorders. *Acta Neuropathol* 2009; **117** (2): 215–216.

19. Duda JE, Shah U, Arnold SE, Lee VM, Trojanowski JQ. The expression of alpha-, beta-, and gamma-synucleins in olfactory mucosa from patients with and without neurodegenerative diseases. *Exp Neurol* 1999; **160**: 515–522.

20. Arnold SE, Lee EB, Moberg PJ *et al.* Olfactory epithelium amyloid-beta and paired helical filament-tau pathology in Alzheimer disease. *Ann Neurol* 2010; **67**: 462–469.

21. Witt M, Bormann K, Gudziol V *et al.* Biopsies of olfactory epithelium in patients with Parkinson's disease. *Mov Disord* 2009; **24**: 906–914.

22. Fumimura Y, Ikemura M, Saito Y *et al.* Analysis of the adrenal gland is useful for evaluating pathology of the peripheral autonomic nervous system in Lewy body disease. *J Neuropathol Exp Neurol* 2007; **66**: 354–362.

23. Saito Y, Ruberu NN, Sawabe M *et al.* Staging of argyrophilic grains: an age-associated tauopathy. *J Neuropathol Exp Neurol* 2004; **63**: 911–918.

24. Saito Y, Ruberu NN, Sawabe M *et al.* Lewy body-related alpha-synucleinopathy in aging. *J Neuropathol Exp Neurol* 2004; **63**: 742–749.

25. Saito Y, Kawashima A, Ruberu NN *et al.* Accumulation of phosphorylated alpha-synuclein in aging human brain. *J Neuropathol Exp Neurol* 2003; **62**: 644–654.

26. Ikemura M, Saito Y, Sengoku R *et al.* Lewy body pathology involves cutaneous nerves. *J Neuropathol Exp Neurol* 2008; **67**: 945–953.

27. McKeith IG, Galasko D, Kosaka K *et al.* Consensus guidelines for the clinical and pathologic diagnosis of dementia with Lewy bodies (DLB): report of the consortium on DLB international workshop. *Neurology* 1996; **47**: 1113–1124.

28. Folstein MF, Folstein SE, McHugh PR. 'Mini-mental state'. A practical method for grading the cognitive state of patients for the clinician. *J Psychiatr Res* 1975; **12**: 189–198.

29. Hasegawa K Inoue K, Moriya K. An investigation of dementia rating scale for the elderly. *Seishin Igaku* 1974; **16**: 965–969.

30. Hosokawa T, Yamada Y, Isagoda A, Nakamura R. Psychometric equivalence of the Hasegawa Dementia Scale-Revised with the Mini-Mental State Examination in stroke patients. *Percept Mot Skills* 1994; **79**: 664–666.

31. Lawton MP, Brody EM. Assessment of older people: self-maintaining and instrumental activities of daily living. *Gerontologist* 1969; **9**: 179–186.

32. Morris JC. The Clinical Dementia Rating (CDR): current version and scoring rules. *Neurology* 1993; **43**: 2412–2414.

33. McKhann G, Drachman D, Folstein M, Katzman R, Price D, Stadlan EM. Clinical diagnosis of Alzheimer's disease: report of the NINCDS-ADRDA Work Group under the auspices of Department of Health and Human Services Task Force on Alzheimer's Disease. *Neurology* 1984; **34**: 939–944.

34. McKeith IG, Dickson DW, Lowe J *et al.* Diagnosis and management of dementia with Lewy bodies: third report of the DLB Consortium. *Neurology* 2005; **65**: 1863–1872.

35. Gallyas F. Silver staining of Alzheimer's neurofibrillary changes by means of physical development. *Acta Morphol Acad Sci Hung* 1971; **19**: 1–8.

36. Fujiwara H, Hasegawa M, Dohmae N *et al.* alpha-Synuclein is phosphorylated in synucleinopathy lesions. *Nat Cell Biol* 2002; **4**: 160–164.

37. Braak H, Braak E. Neuropathological stageing of Alzheimer-related changes. *Acta Neuropathol* 1991; **82**: 239–259.

38. Braak H, Alafuzoff I, Arzberger T, Kretzschmar H, Del Tredici K. Staging of Alzheimer disease-associated neurofibrillary pathology using paraffin sections and immunocytochemistry. *Acta Neuropathol* 2006; **112**: 389–404.

39. Murayama S, Saito Y. Neuropathological diagnostic criteria for Alzheimer's disease. *Neuropathology* 2004; **24**: 254–260.

40. Consensus recommendations for the postmortem diagnosis of Alzheimer's disease. The National Institute on Aging, and Reagan Institute Working Group on Diagnostic Criteria for the Neuropathological Assessment of Alzheimer's Disease. *Neurobiol Aging* 1997; **18**: S1–S2.

41. Hyman BT, Trojanowski JQ. Consensus recommendations for the postmortem diagnosis of Alzheimer disease from the National Institute on Aging and the Reagan Institute Working Group on diagnostic criteria for the neuropathological assessment of Alzheimer disease. *J Neuropathol Exp Neurol* 1997; **56**: 1095–1097.

42. Jellinger KA. Dementia with grains (argyrophilic grain disease). *Brain Pathol* 1998; **8**: 377–386.

43. Jellinger KA, Bancher C. Senile dementia with tangles (tangle predominant form of senile dementia). *Brain Pathol* 1998; **8**: 367–376.

44. Kosaka K. Diffuse neurofibrillary tangles with calcification: a new presenile dementia. *J Neurol Neurosurg Psychiatry* 1994; **57**: 594–596.

45. Hawkes CH, Doty RL. *The Neurology of Olfaction*. Cambridge, UK: Cambridge University Press, 2009; 16–21.

46. Hawkes CH, Del Tredici K, Braak H. Parkinson's disease: a dual-hit hypothesis. *Neuropathol Appl Neurobiol* 2007; **33**: 599–614.

47. Graziadei PP, Okano M. Neuronal degeneration and regeneration in the olfactory epithelium of pigeon following transection of the first cranial nerve. *Acta Anat (Basel)* 1979; **104**: 220–236.

48. Graziadei PP, Monti Graziadei AG. Regeneration in the olfactory system of vertebrates. *Am J Otolaryngol* 1983; **4**: 228–233.

49. Ubeda-Bañon I, Saiz-Sanchez D, de la Rosa-Prieto C, Argandoña-Palacios L, Garcia-Muñozguren S, Martinez-Marcos A. alpha-Synucleinopathy in the human olfactory system in Parkinson's disease: involvement of calcium-binding protein- and substance P-positive cells. *Acta Neuropathol* 2010; **119**: 723–735.